Molecular Structure and Orientation of Gel-Spun Polyethylene Fibers

Ismail Karacan

Department of Textile Engineering, Faculty of Engineering, Erciyes University, TR-38039 Kayseri-Turkey

Received 10 January 2005; accepted 17 November 2005
DOI 10.1002/app.22952
Published online 17 April 2006 in Wiley InterScience (www.interscience.wiley.com).

ABSTRACT: Characterization of molecular structure and orientation of six commercially available gel-spun polyethylene fibers have been carried out using infra-red and Raman spectroscopy, thermal and X-ray diffraction analysis, together with optical microscopy techniques. Thermal and X-ray diffraction analysis revealed the existence of highly oriented orthorhombic and monoclinic crystallites together with a highly oriented intermediate phase known as pseudohexagonal mesophase structure. The results suggest the existence of a three-phase structure consisting, at room temperature, of orthorhombic and monoclinic polymorphic crystallites, oriented noncrystalline and un-oriented noncrystalline (amorphous) phases, respectively. The crystallinity measurements have been carried out using density, thermal and X-ray diffraction analysis together with infra-red and Raman spectroscopy techniques whereas the molecular orientation measurements have been carried out using birefringence and polarized IR spectroscopy, respectively. The results obtained from density, thermal analysis, and Raman spectroscopy based on a simple two-phase modeling approach lead to the overestimated amorphous fractions and appears to ignore the presence of an intermediate phase known as oriented noncrystalline structure. X-ray analysis has also been used for the measurement of the apparent crystallite sizes. The birefringence values have been used to determine the overall orientation parameters whereas the dichroic measurements of IR bands have been used to determine the crystalline and oriented noncrystalline orientation parameters. The results show that the orthorhombic and monoclinic phases are more highly oriented than the oriented pseudohexagonally packed noncrystalline chains.
© 2006 Wiley Periodicals, Inc. J Appl Polym Sci 101: 1317–1333, 2006

Key words: gel-spun polyethylene; orientation; crystallinity; infrared and Raman spectroscopy; thermal analysis; birefringence; X-ray diffraction

INTRODUCTION

The development and commercial introduction of organic and inorganic high performance fibers has been one of the success stories of the last few decades. These fibers are playing an increasingly important role in demanding environments such as aerospace, military, and industrial applications. Because of their desirable properties such as high strength, high modulus, and excellent resistance to a wide range of chemicals, these fibers are finding applications as ballistic protection vests, protective gloves, wires and cables in nuclear plants, and structural composites with carbon fibers in aerospace industry.

It is generally known that linear-flexible polymers, when molten, consist of entangled random coils. Keller[1] has demonstrated that such conventional polymers form folded crystals. Fibers produced from these polymers by conventional spinning, followed by drawing (draw ratios up to 10), still contain a large proportion of molecular chains in a folded conformation. Consequently, one of the approaches to the production of high performance fibers has been in the direction of modifying the morphological structure of linear-flexible chain polymers by superdrawing, solid state extrusion, and gel spinning.

In an attempt to enhance the physical properties of polyethylene, Capaccio and Ward[2–3] have employed the superdrawing method. They showed that, by choosing an appropriate molecular weight distribution and by drawing at a suitable temperature and rate, chain-folded crystallites can be partially unfolded to give chain-extended materials at high draw ratios. Polyethylene fibers with a modulus of around 70 GPa have been produced by this superdrawing technique.

One of the most successful method of development and commercial introduction in the production of high-strength, high-modulus polyethylene is the process of gel-spinning. This process was discovered and patented in Holland by Dutch State Mines (DSM) and in USA by Allied Signal Corp (now part of Honeywell International Inc.). Dutch products are introduced under the trade name of Dyneema® whereas the USA products are introduced under the trade name of Spectra®.[4–6] Honeywell International sees[5] applications based on thermosetting resins and elastomers, while ballistic protection and marine applications

Correspondence to: I. Karacan (ismailkaracan@erciyes.edu.tr).

© 2006 Wiley Periodicals, Inc.

TABLE I
Sample Details

Sample	$n_{/\!/}$	$n_{\perp}$	Δn @ 589.3 (nm)	$\langle\cos^2\theta_{c,f}\rangle$ opt	Diameter (μm)	Density[a] (g/cm^3)	Lorentz Density (g/cm^3)	Tensile[a] Strength (GPa)	Elongation[a] at Break (%)	Young's[a] modulus (GPa)
SPECTRA® 900	1.5900	1.5310	0.0590	0.948	48±1	0.97	0.9735	2.61	3.6	79
SPECTRA®1000	1.5910	1.5320	0.0590	0.948	26±1	0.97	0.9750	3.25	2.9	113
SPECTRA®2000	1.5920	1.5320	0.0600	0.959	24±1	0.97	0.9755	3.25	2.9	116
DYNEEMA®SK60	1.5900	1.5320	0.0580	0.937	20±1	0.97	0.9745	2.7	3.5	89
DYNEEMA®SK65	1.5900	1.5320	0.0580	0.937	24±1	0.97	0.9745	3.0	3.6	95
DYNEEMA®SK75	1.5920	1.5320	0.0600	0.959	18±1	0.97	0.9755	3.4	3.8	107

[a] Manufacturer's data.

such as ropes and high performance sail-cloths are envisaged by DSM.[6]

The gel-spun filaments of polyethylene are reported to be drawn to very high draw ratios, which produce a very highly oriented structure. Values of tensile strength up to 5 GPa and of Young modulus of 120 GPa have been reported[7–8] for polyethylene filaments made in this way.

The molecular structure and properties of polyethylene have been the subject of many interesting and useful studies including X-ray diffraction,[9–15] Optical analysis,[16–17] Thermal analysis,[18–21] NMR,[22–24] Infrared analysis,[25–32] Raman analysis,[33–35] and Mechanical modeling.[36] In particular, Hsieh and Hu,[10] using high-temperature wide-angle X-ray diffraction method, showed that the tension along the fiber axis direction encourages the structural transformation from the orthorhombic to the monoclinic phase. Mahendrasingam et al.,[11] using wide-angle and small-angle X-ray diffraction methods, showed the formation of the orthorhombic and the intermediate hexagonal structures. They showed that the first observable crystals are highly oriented orthorhombic form, with increasing draw ratios additional crystallization in the hexagonal form is observed. In a separate investigation, Fu et al.,[15] using full-pattern X-ray analysis, suggested the presence of three phase structure consisting of crystalline, amorphous, and oriented intermediate phases. This study showed the lack of lateral order in the oriented intermediate phase accounting for a proportion of 30% of the total mass of the Spectra® 900 fiber. Hamza and coworkers,[17] using optical microscopy method, measured the refractive index profile of drawn polyethylene fibers. In a series of publications, Wunderlich and coworkers,[18–20] using thermal analysis, showed that the crystalline phase of gel-spun polyethylene fibers is polymorphic in character, consisting of large proportion of orthorhombic structure followed by a small proportion of oriented intermediate structure known as pseudohexagonal mesophase. It has also been shown that when the polyethylene fibers are longitudinally or laterally constrained, large amounts of hexagonal structures are formed. Annealing experiments[18] carried out at 100°C showed no detectable structural changes as observed by Atomic Force Microscopy and Small-Angle X-ray scattering experiments despite considerable loss of mechanical properties. SAXS experiments[18] also showed no presence before annealing or formation after annealing of folded-chain crystals down to thickness region of 5 nm.

Using ultraviolet-visible dichroism of dyed polyethylene films, Kaito et al.[27] obtained amorphous orientation parameter and found that the orientation parameter of amorphous structure decreases with decreasing length of dye molecules. Lu et al.[33] used Raman microscopy to analyze a series of high modulus polyethylene fibers and their measurements of the 1131:1064 cm^{-1} band intensity ratios are related to the Young's modulus of the fibers. Using online Raman spectroscopy, Paradkar et al.,[34] obtained fractional crystallinity values using normalized integrated intensity of a crystalline band located at 1418 cm^{-1}.

In the present investigation, commercially available gel-spun polyethylene fibers have been studied with the aim of characterizing the structural parameters in terms of the degree of crystallinity, crystallite size, and the molecular orientation of the crystalline and noncrystalline chains with the ultimate aim of gaining an enhanced understanding of the processing-structure-property relationships.

EXPERIMENTAL

Materials

Samples used in the present study were three grades of gel-spun PE fibers commercially produced by Dutch State Mines (DSM) of Holland and Allied Signal (now part of Honeywell International Inc.) of USA. Totally six samples with molecular weights greater than 10^6 Daltons were used in the study. Details of the samples showing the refractive indices, birefringence, $\cos^2\theta_{c,f\text{opt}}$, diameter, density, Lorentz density, and me-

chanical properties can be found in Table I where the samples have been identified by their commercial name. Unfortunately, the processing conditions were not made available by the manufacturers due to commercial reasons.

Refractive index measurements

The refractive indices of the fiber samples with the aim of determining birefringence values were measured using an image splitting Carl Zeiss Jena interphako interference microscope. The refractive indices in the fiber axis direction ($n_{//}$) and transverse direction ($n_{\perp}$) were measured by matching the refractive index of Cargille immersion liquids. The refractive indices of Cargille liquids are accurate to ± 0.0002 in the 1.3–1.7 refractive index region. The birefringence of a fiber sample can be defined as the difference between the refractive index for light polarized parallel to the fiber axis, $n_{//}$, and that for light polarised perpendicular to the fiber axis, $n_{\perp}$. The measured values of the refractive indices and the birefringences are shown in Table I.

Infra-red measurements

An IR-Plan® microscope installed on a Nicolet Magna IR 750 Fourier Transform spectrophotometer equipped with a ZnSe based wire grid polarizer was employed for infra-red dichroic measurements. The IR-plan® microscope allows the single fibers to be examined. An average of 10 single filaments were studied to maintain the reproducibility of the results.

The directly measured absorbance values were subject to inaccuracies due to the polarizer transmission of a small fraction of radiation polarized perpendicularly to its principal transmission direction. These inaccuracies can be corrected according to a procedure developed by Green and Bower.[37] In previous work on highly oriented polypropylene[38] and PVC films[39] and Polyacrylonitrile (PAN)-based acrylic fibers,[40] such corrections were found to be very small for absorbance values less than 1.5 and insignificant for samples with low orientation.

In all cases, 200 interferograms of a sample were averaged and transformed with Happ–Genzel apodization function. All the spectra were collected at a resolution of 2 cm^{-1}. Finally, all the spectra were analyzed using the OMNIC® software provided by the spectrometer and curve fitting procedures where appropriate.

Raman measurements

A Nicolet 950 Fourier Transform Raman spectrometer was used for collecting the spectra of the fiber specimens. In all cases, 250 scans with a resolution of 4 cm^{-1} was employed. Depolarized laser was used for the data collection because of the orientation independent data requirement. Initial data analysis was carried out with the use of OMNIC® software followed by curve fitting procedures[41] assuming a combined Gaussian and Lorentzian peak profiles. The peak areas were used as integrated intensities.

DSC measurements

The differential scanning calorimetry (DSC) experiments were carried out using a DuPont Differential Scanning Calorimeter controlled by a Thermal Analyst 2000 system. Typical sample weights used were approximately 5 mg. The heating rate of 20°C/min and an upper temperature range of 200°C were selected. Indium (m.p. 156.5°C) was used as a calibration standard. The specimens were always tested in a nitrogen environment.

X-ray diffraction

The wide-angle X-ray diffraction traces were obtained using Scintag® X-ray diffractometer system utilizing nickel filtered CuK_{α} radiation (wavelength of 1.542 Å) and voltage and current settings of 50 kV and 40 mA, respectively. Counting was carried out at 20 steps per degree. The observed equatorial X-ray scattering data in the $10-60°$ 2θ range was corrected for Lorentz, polarization, and incoherent scatter effects; they were then normalized to a convenient standard area. Intensity corrected and normalized X-ray data were analyzed by the peak fitting procedure detailed earlier.[41]

The peak widths at half-height have been corrected using the Stoke's deconvolution procedure.[42] Finally, the apparent crystallite size of a given reflection was calculated using the Scherrer equation:

$$L(\mathrm{hkl}) = \frac{K\lambda}{\beta\cos(\theta)} \tag{1}$$

where θ is the Bragg angle for the reflection concerned, λ is the wavelength of radiation (1.542 Å), L(hkl) is the mean length of the crystallite perpendicular to the planes (hkl), β is either the integral breadth or the breadth at half maximum intensity in radians, and K is a Scherrer parameter.

Analysis of experimental data

Infra-red data—curve fitting

In the present work, the parallel and perpendicular polarization spectra were fitted independently, allowing the peak positions and peak widths to vary freely, using the peak positions previously found using OMNIC® software as a guide to the starting values. Finally, the peak positions and the peak widths obtained

from the two spectra were averaged and the parallel and perpendicular spectra were refitted, fixing the positions and the widths at these average values and allowing only the peak heights to vary.

Infra-red data—evaluation of orientation averages

For uniaxially oriented systems with cylindrical symmetry such as fibers, the calculation of orientation averages derived from the infra-red data analysis can be carried out with the use of the dichroic ratio as defined:

$$D = A_{/\!/}/A_{\perp} \tag{2}$$

where $A_{//}$ and $A_{\perp}$ are the measured absorbance values for radiation polarized parallel and perpendicular to the fiber axis, respectively. To a good approximation, the dichroic ratio is related to the orientation parameter $\langle P_2(\cos\theta)\rangle$ by

$$\langle P_{200}\rangle = \langle P_2(\cos\theta)\rangle = \frac{D-1}{D+2}\cdot\frac{D_0+2}{D_0-1} \tag{3}$$

where θ is the angle between the chain axis and the fiber axis, and $D_0 = 2\cot^2\alpha$, α being the angle between the transition moment associated with the vibrational mode and the chain axis. In this work, it is assumed that the polyethylene chains have no preferred orientation around their own axis. For samples with very low birefringence, such as the present polyethylene fiber samples, eqs. (2) and (3) are, however, sufficiently accurate. The $\langle P_2(\cos\theta)\rangle$ is known as the second-order Legendre polynomial and is also known as the Herman's orientation factor in polymer and fiber science.

The values of $\langle P_2(\cos\theta)\rangle$ for peaks located at 730, 719, 718, and 717 cm^{-1}, showing perpendicular polarization characteristics, assuming a transition moment angle of 90°, are calculated by eq. (3).

Because of the difficulties in understanding the precise meaning of a particular set of numerical values of $<P_{200}>$, they are converted into values of $\langle\cos^2\theta_{c,f}\rangle$ where $\theta_{c,f}$ is the angle between the chain and the fiber axis direction. The corresponding values of $\langle\cos^2\theta_{c,f}\rangle$ are determined by the eq. (4):

$$\langle\cos^2\theta_{c,f}\rangle = \frac{1}{3}(1 + 2\langle P_{200}\rangle) \tag{4}$$

$<\cos^2\theta_{c,f}>$ may vary between 0 and 1. For random orientation, $<\cos^2\theta_{c,f}>$ may take the value of 1/3, while for complete orientation the value of $\langle\cos^2\theta_{c,f}\rangle$ is 1.

Evaluation of orientation averages from refractive indices

For a transversely isotropic sample, such as uniaxially oriented fiber, the measured refractive indices can be used to calculate optical orientation averages by using the following general equations.[43]

$$\frac{\phi_{/\!/} - \phi_{\perp}}{\phi_{/\!/} + 2\phi_{\perp}} = \frac{2\Delta\alpha}{3\alpha_0}P_{200} \tag{5}$$

$$\phi_i = \frac{n_i^2 - 1}{n_i^2 + 2} \tag{6}$$

Substituting the expressions for ϕ_i (where i is either // or $\perp$) from eq. (6) into eq. (5) and writing $\Delta n = n_{//} - n_{\perp}$ and $n_{iso} = \frac{1}{3}(n_{//} + 2n_{\perp})$ then leads, to a good approximation, to

$$P_{200} = \left(\frac{3\alpha_0}{\Delta\alpha}\right)\frac{2n_{iso}\Delta n}{(n_{iso}^4 + n_{iso}^2 - 2)} \tag{7}$$

where $n_{//}$ is the refractive index parallel to the fiber axis direction and $n_{\perp}$ is the refractive index perpendicular to the fiber axis direction.

In the present study, a value of 0.064 has been used as the maximum birefringence value for the fully oriented sample of polyethylene.[16] Substituting $P_{200} = 1$ in eq. (7), together with the experimental value of n_{iso}, leads to $\frac{3\alpha_0}{\Delta\alpha} = 31.5 \pm 0.2$. Using this value and eq. (7), the values of P_{200} can be determined from the refractive index data shown in Table I. From P_{200}, the values of $\langle\cos^2\theta_{c,f}\rangle$opt can be determined using eq. (8), and the results for the samples are shown in Table I.

$$\langle\cos^2\theta_{c,f}\rangle_{opt} = \frac{1}{3}(1 + 2\langle P_{200}\rangle) \tag{8}$$

Evaluation of crystallinity from depolarized raman spectrum

The integrated areas of Raman bands can be used for the determination of the fractional crystallinity of the PE fiber samples.[34] The integrated area of the Raman twisting bands in the 1295–1305 cm^{-1} region can be used as an internal band to normalize Raman intensities.[34] The normalized peak area of crystalline Raman band positioned at 1418 cm^{-1} has been used to determine the fractional crystallinity of the polyethylene fiber samples. For the fully crystalline PE sample a value of 0.44 as a normalized integrated intensity of 1418 cm^{-1} Raman crystalline band was determined by Paradkar et al.[34] and the same value has been used in the present investigation. The Raman crystallinity of

polyethylene fiber samples can be directly determined using the integrated peak area (I_{1418}) of crystalline Raman peak located at 1418 cm^{-1}, according to the eq. (9)

$$\chi_T = \frac{I_{1418}}{I_\gamma \times 0.44} \times 100(\%) \quad (9)$$

where I_T is the integrated peak area of the twisting bands located in the 1295–1305 cm^{-1} region. This calculation assumes that the fiber structure is based on a two-phase modeling consisting of crystalline and amorphous phases, respectively.

Evaluation of fractional crystallinity from density values

Assuming a two-phase model consisting of crystalline and noncrystalline (amorphous) phase, fractional crystallinity (χ_c) using density values can be determined using eq. (10)

$$\chi_c = \frac{\rho_c}{\rho}\left(- \frac{\rho - \rho_a}{\rho_c - \rho_a}\right) \times 100(\%) \quad (10)$$

where ρ is the sample density and ρ_a is the density of the amorphous material given by Kaito et al.[27] as 0.8525 g/cm^3 whereas ρ_c is the density of the fully crystalline material taken as 1.01 g/cm^3 determined in the present investigation. Because of the limitation of the assumption of a two-phase structure, the results shown in Table VII ignores the presence of intermediate phase leading to high values of amorphous fraction ($1-\chi_c$).

According to Vries,[16] density (ρ) can be calculated using the relation in eq. (11) based on well-known Lorentz-Lorenz relationship:

$$\rho = K\left[\frac{n_{\text{iso}}^2 - 1}{n_{\text{iso}}^2 + 2}\right] \quad (11)$$

where n_{iso} is defined as the isotropic refractive index determined from eq. (12)

$$n_{\text{iso}} = \frac{1}{3}(n_{/\!/} + 2n_\perp) \quad (12)$$

Using eqs. (11) and (12), density of the PE fiber samples can be estimated. The constant K is given by Vries[16] as 3.053 for fully oriented PE samples.

Evaluation of DSC crystallinity from melting enthalpy values

Assuming a two-phase model consisting of crystalline and amorphous phases, the degree of DSC crystallinity can be evaluated from the melting enthalpies using eq. (13)

$$\chi_c = \frac{\Delta H_m}{\Delta H_m^0} \times 100\% \quad (13)$$

where χ_c is the degree of crystallinity evaluated by d.s.c. method, ΔH_m is the melting enthalpy of the sample and ΔH_m° is the melting enthalpy of 100% crystalline sample and is taken as 293 J/g as published in the literature.[21] It is clear that the two-phase model assumes constant amorphous density in highly oriented samples while disregarding the presence of oriented intermediate phase.

Evaluation of X-ray crystallinity

X-ray crystallinity[44] is based on the ratio of the integrated intensity under the resolved peaks to the integrated intensity of the total scatter under the experimental trace. This definition can be expressed as in eq. (14)

$$\chi_c = \frac{\int_0^\infty I_{\text{cr}}(2\theta)d(2\theta)}{\int_0^\infty I_{\text{tot}}(2\theta)d(2\theta)} \quad (14)$$

The area under the background is considered to correspond to the un-oriented noncrystalline scatter (i.e., amorphous scatter). It should be emphasized that X-ray crystallinity is defined between two arbitrarily chosen angles and should be considered as an optimum mathematical solution.

Evaluation of crystallinity through the estimation of trans conformer content

The infra-red crystallinity through the evaluation of the total trans conformer content in the crystalline phase is calculated using eq. (15)

$$\chi_{\text{trans}} = \frac{\sum A_{0,\text{trans}}}{\sum A_{\text{o,trans}} + \sum A_{\text{o,non-crystalline}}} \times 100\% \quad (15)$$

where $\Sigma A_{0,\text{trans}} = A_{//\text{trans}} + 2A_{\perp\text{trans}}$ and $\Sigma A_{0,\text{noncrystalline}} = A_{//\text{noncrystalline}} + 2A_{\perp\text{noncrystalline}}$, respectively. $A_{//\text{trans}}$ and $A_{\perp\text{trans}}$ are the absorbance values of trans bands showing parallel and perpendicular polarization characteristics and so on. $\Sigma A_{0,\text{trans}}$ is the sum of the absorbance values of trans bands located at 730 and 717 cm^{-1} in the crystalline phase whereas $\Sigma A_{0,\text{noncrystalline}}$ is based on the absorbance values of IR

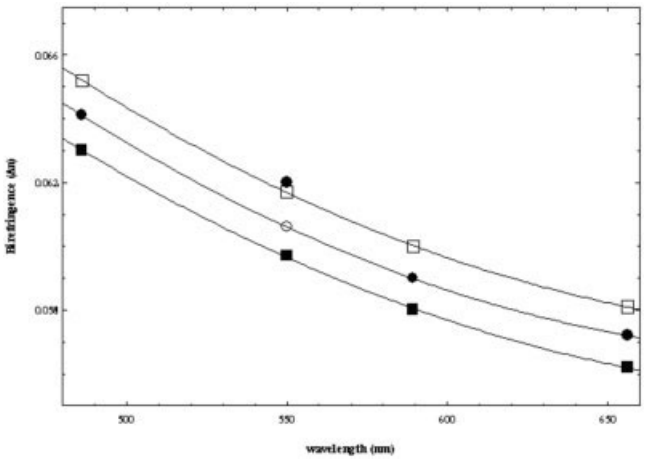

Figure 1 The variation of birefringence (Δn) with wavelength of light used. ■, Dyneema® SK60/Dyneema® SK65; ●, Spectra® 900; ○, Spectra® 1000; □, Spectra® 2000/ Dyneema® SK75.

band located at 719 cm^{-1} in the oriented noncrystalline phase.

RESULTS AND DISCUSSION

Orientation measurements: analysis of the refractive index and birefringence data

The measured refractive indices and the birefringence values of all samples at a wavelength of 589.3 nm are listed in Table I. The measurements of refractive indices are carried out at the wavelengths of 486.1, 546.1, 589.3, and 656.3 nm, respectively. Figure 1 shows the variation of birefringence as a function of wavelength of light used during the experiments. According to this figure, the birefringence values decrease with increasing wavelength. This behavior is known to be due to the spectral dispersion.

The measured birefringence (Δn) and $\langle\cos^2\theta_{c,f}\rangle$opt values listed in Table I show that the polyethylene fiber samples possess very high degrees of chain alignment along the fiber axis direction. It shows that the overall orientation parameter in terms of $\langle\cos^2\theta_{c,f}\rangle$opt values varies between 0.937 and 0.959, respectively. Normally, the orientation parameters obtained from optical microscopy via the birefringence measurements are considered to be due to the overall molecular orientation of the crystalline and noncrystalline (i.e., amorphous) phases, respectively. With this method it is not possible to have access to the orientation parameter of either the crystalline, oriented noncrystalline (i.e., intermediate phase between crystalline and amorphous phase) or the amorphous phases directly, unlike the other methods including the X-ray and IR spectroscopy method used in the present study.

The results suggest that Spectra® 2000 and Dyneema® SK75 grade fiber samples have almost perfect overall orientation as shown by their high $<\cos^2\theta_{c,f}>_{opt}$ values shown in Table I.

Analysis of infra-red spectroscopy data

The IR spectrum of polyethylene in the 3200–650 cm^{-1} region shows six well-defined IR peaks. Of these peaks, those at 2920, 2850 cm^{-1} can be described as very strong in intensity and showing perpendicular polarization characteristics, where as the peaks at 1473, 1463, 730, and 718 cm^{-1} can be described as medium in intensity and also show perpendicular polarization characteristics.

Because of the complications arising from highly absorbing bands in the 3000–2800 cm^{-1} and 1550–1350 cm^{-1} regions, the analysis has been limited to the doublet in the 775–675 cm^{-1} region, presented in Figure 2. This region is also more attractive for quantitative analysis because of the low absorbance values and the absence of imperfect polarizer related complications.

During the curve fitting procedures, it was found necessary to resolve the peak at 718 cm^{-1} into two peaks, with positions of 719 cm^{-1} and 717 cm^{-1} to improve the fitting. The position of the IR peak often referred to in the literature as 720 cm^{-1} has been found to be 718 cm^{-1} after the curve fitting. The peak at 718 cm^{-1} has been quoted in the literature[25] as arising from a combination of crystalline and noncrystalline (amorphous) phases.

The second derivative spectrum (Fig. 3) of the 720–710 cm^{-1} region also gave two minima with the similar positions of 717 and 719 cm^{-1}, respectively. As shown in Figure 4, splitting of the 718 cm^{-1} IR peak

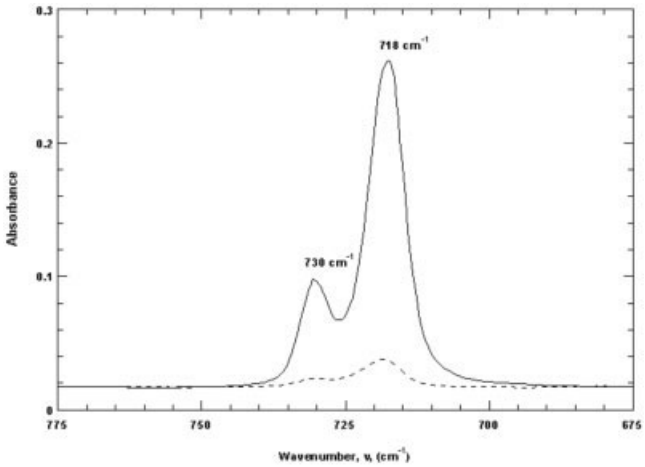

Figure 2 A typical IR spectrum of polyethylene in the CH_2 rocking region (775–675 cm^{-1} region). Solid line corresponds to the perpendicular polarization. Broken line corresponds to the parallel polarization direction.

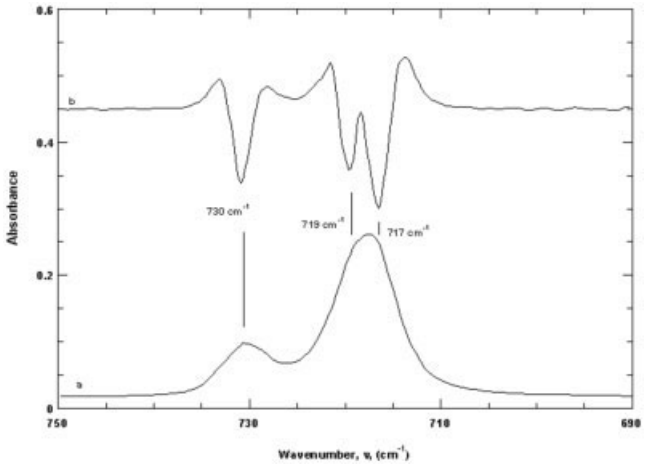

Figure 3 (a) A typical IR spectrum of polyethylene in the 775–675 cm^{-1} region; (b) The second derivative spectrum. The peak positions shown correspond to the minima of the second derivative spectrum.

into 717 and 719 cm^{-1} bands has resulted in a better curve fitting. An additional peak with a position of 726 cm^{-1} was necessary for the best fitting but is not considered further.

730 cm^{-1} peak

The bandwidth of this peak varies between 5 and 6.5 cm^{-1} in the spectral region studied. It has been assigned to in-phase CH_2 rocking modes for the two chains in the orthorhombic unit cell and in crystals of *n*-paraffins. It has been found to be polarized along the *a*-axis of the crystal.[25,26]

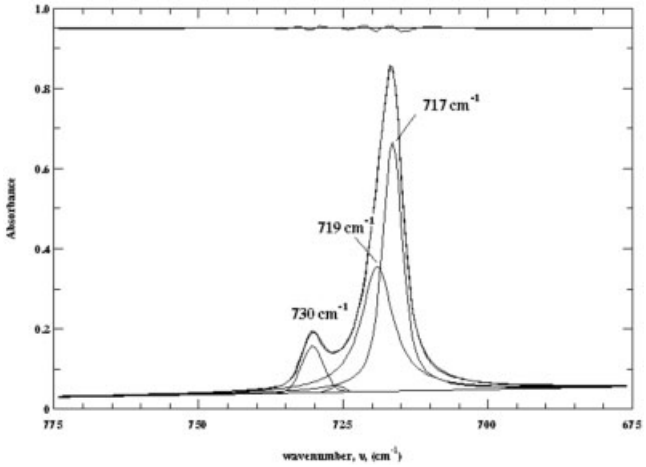

Figure 4 An example of the IR spectrum peak resolution (perpendicular spectrum for Dyneema® SK65 grade sample). The lower curves are the fitted peaks, the middle curve is the observed spectrum, and the upper curve is the difference between the observed spectrum and the fitted spectrum on the same scale.

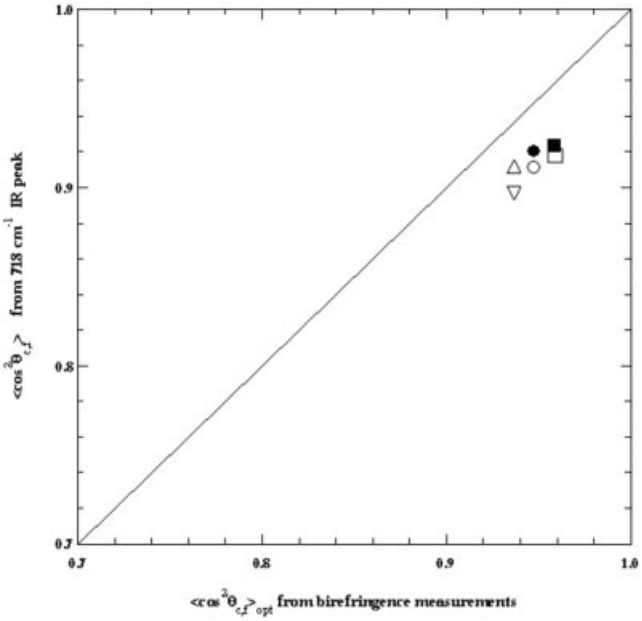

Figure 5 Comparison of $<\cos^2\theta_{c,f}>$ values obtained from the birefringence measurements with those obtained from the 718 cm^{-1} IR peak: ●, Spectra® 900; ○, Spectra® 1000; □, Spectra® 2000; ▽, Dyneema® SK60, ■, Dyneema® SK65; △, Dyneema® SK75

718 cm^{-1} peak

The bandwith of this peak varies between 7.5 and 8 cm^{-1} in the spectral region and has components because of both the crystalline and noncrystalline (amorphous) phases. The crystalline component located at 717 cm^{-1} arises from out of phase CH_2 rocking modes for the two chains in the unit cell.

According to the published literature,[26–32] the crystalline component of this peak arises from the monoclinic structure. The noncrystalline component located at 719 cm^{-1} is assigned to CH_2 rocking modes of the chain segments in the trans conformation.[25,26] Both the crystalline and noncrystalline components of 718 cm^{-1} peak has transition moments perpendicular to the chain axis.

Because of the contributions from the crystalline and noncrystalline phases, the orientation parameters obtained from this peak can be regarded as the average orientation of the crystalline and noncrystalline phases. In this respect, Figure 5 shows the comparison of the orientation parameters ($<\cos^2\theta_{c,f}>_{718}$) obtained from this peak with the overall orientation parameters obtained from the refractive index data. The $<\cos^2\theta_{c,f}>$ values from this peak are slightly less than those from the refractive index data. This may be due to the value of the maximum birefringence used and the transition moment angle assumed as 90°. Any deviation from these assumed values is likely to change the calculated values in consideration.

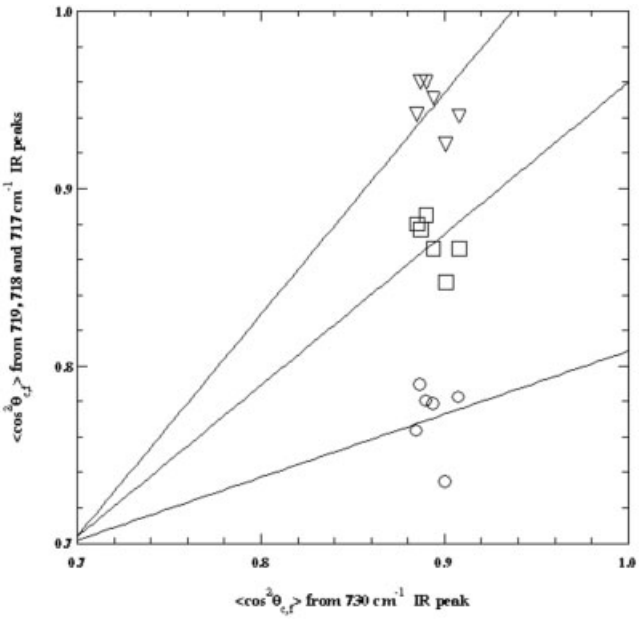

Figure 6 Comparison of $<\cos^2\theta_{c,f}>$ values obtained from the 730 cm^{-1} IR peak with those obtained from 719 (○), 718 (□), and 717 (▽) cm^{-1} infra-red peaks.

717 cm^{-1} peak

This peak is the narrowest peak in the 775–675 cm^{-1} region studied (4.5–5.0 cm^{-1}). It has been assigned to the out of phase CH_2 rocking modes in the monoclinic structure. Transition moment of this peak is perpendicular to the chain axis and a value of 90° is tentatively used as the transition moment angle. This peak has the highest orientation parameter compared with the orientation parameter obtained from the 730 cm^{-1} peak. It shows that the monoclinic structure is slightly more oriented along the fiber axis than the orthorhombic structure.

A recent investigation[31] indicated that stress impacts such as orientation due to drawing may encourage the formation of monoclinic structures. It has been suggested[31] that in the orthorhombic crystalline form, all-trans zigzag planes of polyethylene chains are perpendicular to each other and in the monoclinic crystalline form, all-trans zigzag planes of polyethylene chains are parallel to each other

719 cm^{-1} peak

The bandwidth of this peak varies between 5 and 7.3 cm^{-1}, respectively. This peak is the noncrystalline component of the peak located at 718 cm^{-1} and has been assigned to CH_2 rocking modes of chain segments in trans conformation. According to Snyder,[29] this peak is associated with the sequences of more than four trans bonds and is regarded as arising from a highly oriented hexagonal mesophase. Transition moment of this peak is also perpendicular to the chain axis and shows perpendicular polarization characteristics. As shown in Figure 6, the orientation parameter of this peak, as expected, because of the nature of the hexagonal mesophase, is lower than the orthorhombic and monoclinic structures.

Characterization of molecular structure and crystallization

Analysis of wide angle X-ray diffraction data

Wide-angle X-ray diffraction studies have been carried out with the aim of determining structural parameters in terms of crystallinity and crystallite sizes of the samples studied. As shown in Figure 7, the equatorial traces in the 15–60° 2θ region show two strong (110 and 200), two medium (020 and 310), and six weak (210, 120, 220, 400, 320, and 130) reflections. Figures 8 and 9 show the peak resolution of Spectra® and Dyneema® grade polyethylene fibers. Peak resolutions reveal the *d*-spacings of 110, 200, and 020 reflections as 4.08 ± 0.02 Å, 3.66 ± 0.03 Å, and 2.47 ± 0.02 Å, respectively. The results suggest an orthorhombic unit cell with average basal plane dimensions of $a = 7.32 \pm 0.03$ Å and $b = 4.94 \pm 0.02$ Å.

Table II shows the unit cell dimensions of the orthorhombic structure and the corresponding crystalline density values published in the literature. The average orthorhombic unit cell dimensions of the samples investigated in the present study are slightly smaller than those previously published values indicating closer packing and more perfect lateral arrangement of polyethylene chains. Assuming the *c*-axis dimension of the orthorhombic unit cell as $c = 2.55$ Å,

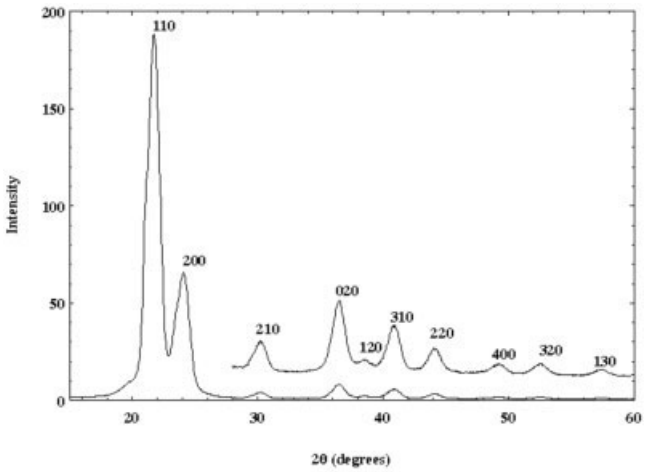

Figure 7 A typical equatorial wide-angle X-ray diffraction trace (15–60° 2θ) of gel-spun polyethylene fiber. The indexing of the reflections corresponds to the orthorhombic unit cell. The upper trace is the magnified version of 28–60° 2θ region to show the relative intensities for the sake of clarity.

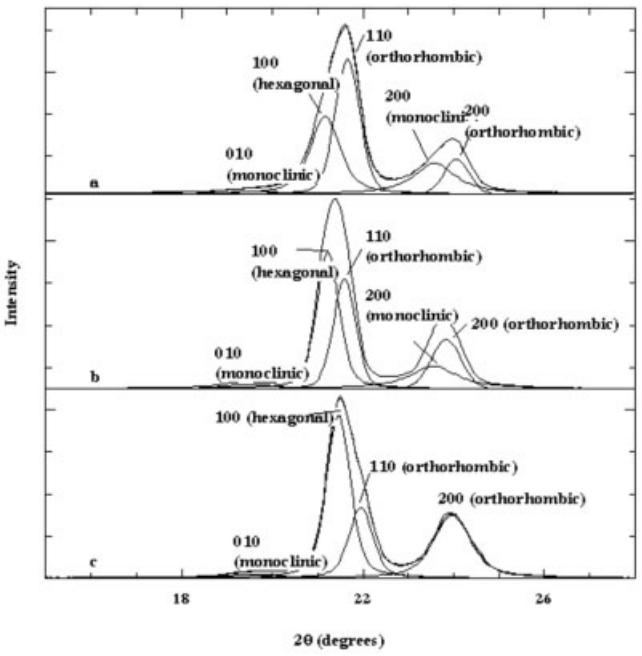

Figure 8 Resolved equatorial diffraction traces of Spectra® grade polyethylene fibers. (a) Spectra® 900; (b) Spectra® 1000; (c) Spectra® 2000. Assignments of the peaks are shown on the traces.

the calculated crystalline density is found to be 1.01 g/cm^3 in good agreement with the published data.[10,12–14] Assuming two chains per unit cell, the chain cross-sectional area for the orthorhombic structure is found to be 18.08 Å^2[22]; in good agreement with the published values showing variation between 17.99 and 18.29 Å^2[22]; as listed in Table II.

The equatorial resolution shows a broad and weak peak with a *d*-spacing of 4.55 ± 0.03 Å assigned to the (010) reflection of the monoclinic structure in the literature.[10,15,20] The peak present as a shoulder to the[200] reflection of the orthorhombic structure with a *d*-spacing of 3.85 ± 0.02 Å is assigned to the 200 reflection of the monoclinic structure.[10,15] Although the presence of $(\bar{2}10)$ reflection is reported[15] in the compressed PE-fibers obtained from powder X-ray diffraction patterns, no such peak with a *d*-spacing of 3.52 Å (25.3° 2θ) was observed in the equatorial fiber traces (shown in Figs. 7–9) of the samples listed in Table I. It seems that[15] the reflections assigned to the monoclinic phase are more clearly visible and well-defined in the powder and compressed X-ray diffraction patterns than in the fiber patterns. This may explain the reasons why $(\bar{2}10)$ reflection due to monoclinic phase is not observed in the uncompressed fiber diffraction traces of the samples studied in the present investigation.

As a result, in the absence of higher number of reflections, the monoclinic structure can be given the tentative unit cell dimensions[15] of $a = 8.09 \pm 0.02$ Å, $b = 4.79 \pm 0.03$ Å, $c = 2.53$ Å, and $\gamma = 107.9°$. Assuming two chains per unit cell, the tentative chain cross-sectional area for the monoclinic unit cell is found to be 18.43 Å^2.

It shows that the chain cross-sectional area of monoclinic structure is, on average, 2% larger than the chain cross-sectional area of the orthorhombic structure. The similarity between the orthorhombic and the monoclinic chain cross-sectional areas explains the reason why these two crystalline forms can coexist together. Furthermore, monoclinic phase is shown to disappear upon heating[20] before the melting of the orthorhombic structure but is found to increase in proportion on lateral compression.[15] As shown in Table IV, the proportion of monoclinic phase varies between 2.5 and 20% for the USA origin PE fibers whereas the same component varies between 3 and 14% for the Holland origin PE fibers, respectively.

The equatorial peak resolution reveals another additional peak present as a shoulder to the (110) orthorhombic reflection with a *d*-spacing of 4.15 ± 0.05 Å assigned to the (100) reflection of the oriented hexagonal[10,20] mesophase structure. Assuming a tentative hexagonal basal plane dimensions of $a = b = 4.8$ Å, $\gamma = 120°$, the cross-sectional area per chain is then found to be ~20 Å^2 This value, because of the room temperature measurement, is ~10% higher than the chain-cross-sectional area of the orthorhombic phase. During the high-temperature X-ray diffraction studies, Kwon et al.[20] found that the chain cross-sectional area of constrained PE fibers in the oriented hexagonal phase can be 20–25% larger than that of the orthor-

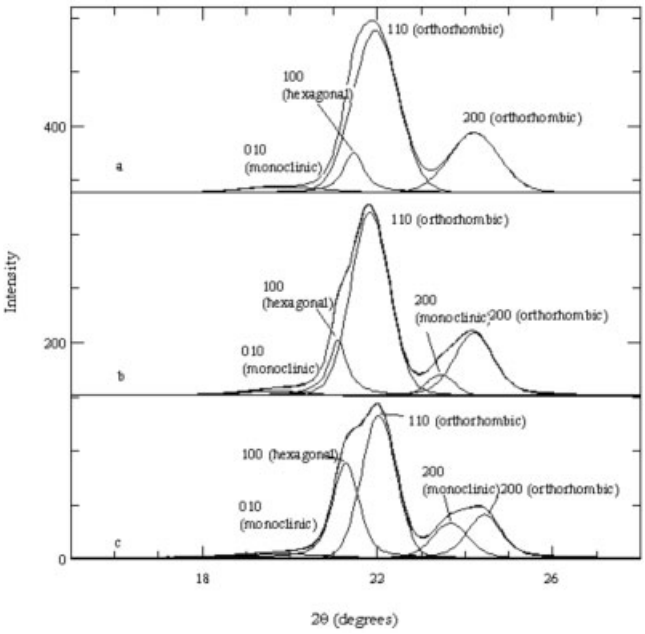

Figure 9 Resolved equatorial diffraction traces of Dyneema® grade polyethylene fibers. (a) Dyneema® SK60; (b) Dyneema® SK65; (c) Dyneema® SK75. Assignments of the peaks are shown on the traces.

TABLE II
Dimensions of the Orthorhombic Unit Cell and the Crystalline Density

a (Å)	b (Å)	c (Å)	ρ_c (g/cm^3)	Cross-sectional area (Å^2)	Reference
7.32 ± 0.03	4.94 ± 0.02	—	1.01	18.08	This work
7.36 ± 0.04	4.89 ± 0.04	2.55	1.02	17.99	10
7.36	4.94	2.534	1.011	18.18	12
7.40	4.93	2.534	1.008	18.24	13
7.406	4.939	2.547	0.9998	18.29	14
7.37	4.90	–	–	18.05	45

hombic structure. This is not a surprising outcome for the hexagonal chains owing to their increased mobility and conformational disorder[20] as well as expected expansion of chain separation processes taking place around the melting region.

It should be noted that the hexagonal phase is defined as an oriented noncrystalline phase, coined an oriented-intermediate phase by Wunderlich and coworkers,[18–20] falling between oriented crystalline and un-oriented noncrystalline (i.e., amorphous) phase and characterized by a noncrystalline structure consisting of chains with highly extended trans conformation along the fiber axis direction, together with poor lateral order because of the large chain separation distances involved.

The crystallite sizes perpendicular to the 110, 200, and 020 planes of the orthorhombic structure are listed in Table III. The crystallite size perpendicular to the 110 planes of the USA based PE fibers varies between 129.8 and 144.8 Å, corresponding up to 35 chains in this direction.

The crystallite size perpendicular to the 200 planes of the USA based PE fibers varies between 86.1 and 126.6 Å corresponding up to 34 chains in this direction.

Also, the crystallite size perpendicular to the 020 planes of the USA based PE fibers varies between 90.3 and 100.4 Å corresponding up to 40 chains. This means than the orthorhombic structure of USA based PE fibers is made from an average of 1360 laterally packed polymer chains.

Using the same approach, the results point to an average number of laterally packed chains of 725 for the Holland based PE fibers. It is clear that the USA based PE fibers tend to have larger laterally packed orthorhombic structures than the Holland based PE fibers.

The X-ray crystallinity of the orthorhombic, monoclinic, and pseudohexagonal (oriented noncrystalline) structures are listed in Table IV where the amorphous phase (unoriented noncrystalline phase) takes the value of around 2–3% for the USA based PE fibers and

TABLE III
X-ray Diffraction Analysis Results

Sample	Indexing	Observed d-spacing (Å)	Peak position (2θ)	Corrected half-height width (2θ°)	$L_{(hkl)}$ crystallite size (Å)
SPECTRA® 900	110	4.103	21.658	0.69	129.8
	200	3.698	24.064	0.71	126.6
	020	2.486	36.127	1.03	90.6
SPECTRA® 1000	110	4.115	21.593	0.62	144.8
	200	3.732	23.841	0.86	104.7
	020	2.476	36.278	0.93	100.4
SPECTRA® 2000	110	4.049	21.953	0.66	135.5
	200	3.712	23.973	1.05	86.1
	020	2.468	36.404	1.03	90.3
DYNEEMA® SK60	110	4.049	21.953	1.40	64.5
	200	3.639	24.208	1.55	58.4
	020	2.449	36.691	1.48	63.1
DYNEEMA® SK65	110	4.071	21.831	1.16	77.6
	200	3.677	24.202	1.17	77.2
	020	2.457	36.572	1.29	72.1
DYNEEMA® SK75	110	4.033	22.037	1.04	86.5
	200	3.642	24.441	1.00	90.0
	020	2.453	36.633	1.42	65.3

TABLE IV
Crystallinity Values Obtained from Curve Fitting of X-ray Diffraction Traces

Sample	$\%\chi_1$ monoclinic phase	$\%\chi_2$ oriented hexagonal	$\%\chi_3$ orthorhombic phase	$\Sigma\ \%\chi_c$ mono + ortho phases	χ_{am} (%) unoriented non-crystalline phase
SPECTRA®900	20	30	47	67	3
SPECTRA®1000	18	37	42	60	3
SPECTRA®2000	2.5	46	49.5	52	2
DYNEEMA®SK60	3	9	81	84	7
DYNEEMA®SK65	9	11	76	85	4
DYNEEMA®SK75	14	25	56	70	5

of around 4–7% for Holland based PE fibers in agreement with the previously published data.[20] It is suggested[15] that the amorphous phase may be located on the surface of the fiber or in the defective regions of the PE fibers with low proportion of amorphous material whereas with higher proportion of amorphous material, the amorphous phase may form amorphous domains between oriented intermediate phase, resulting in the reduction of mechanical properties.

As expected, the dominating structure in all the samples is the orthorhombic crystalline phase together with smaller fractions of the crystalline monoclinic and hexagonal (oriented noncrystalline) structures. The USA based polyethylene fibers appear to have more oriented hexagonal mesophase content showing variation between 30 and 46% than the Holland based polyethylene fibers showing variation between 9 and 25% (Table IV). The differences must be due to the different processing conditions employed during the manufacturing stages. The content of oriented noncrystalline phase is found to be in agreement with the published data.[18] For example, Hu et al.[18] found the oriented noncrystalline content of 30 and 33% for the Spectra® 900 and 2000 fibers, respectively. Kwon et al.,[20] using high-temperature X-ray diffraction analysis, showed the gradual appearance of oriented hexagonal peak with a *d*-spacing of 4.15 ± 0.05 Å in the melting temperature region. This shows that the hexagonal structure consists of long range order in the lateral direction.

Table IV also shows the relative proportion of the monoclinic structure to range between 2.5 and 20% for the USA based PE fibers and between 5 and 14% for the Holland based PE fibers, respectively. In general, the proportion of the monoclinic structure is found to be much smaller than the proportion of orthorhombic structure (see Table IV). Previous studies[15] suggest the transformation of orthorhombic to monoclinic phase following the lateral compression of PE fibers, resulting in almost doubled fraction of monoclinic structure.

High-temperature X-ray diffraction studies[10,20] carried out in the melting region suggest the transformation from orthorhombic to pseudohexagonal structure. Above 145°C, the hexagonal structure is shown[20] to completely disappear in parallel with the disappearance of the hexagonal mesophase endotherm observed around 152–157°C.

Analysis of the thermal analysis data

DSC thermograms of gel-spun PE fibers are well-known to exhibit multiple endothermic peaks.[18–20] Thermograms in the temperature range of 100–190°C presented in Figures 10 and 11 show asymmetric endothermic peaks with a main peak positioned around 150°C followed by another endothermic peak located

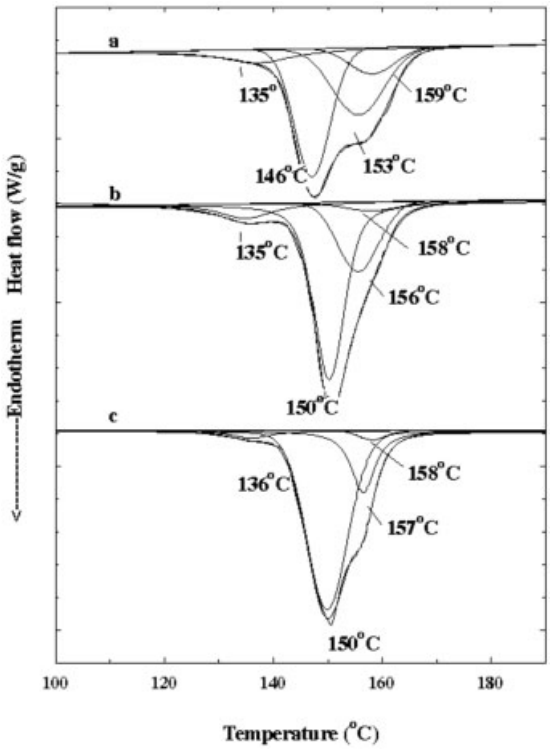

Figure 10 Resolved DSC thermograms of Spectra® grade polyethylene fibers. (a) Spectra® 900; (b) Spectra® 1000; (c) Spectra® 2000. Peak positions are shown on the thermograms.

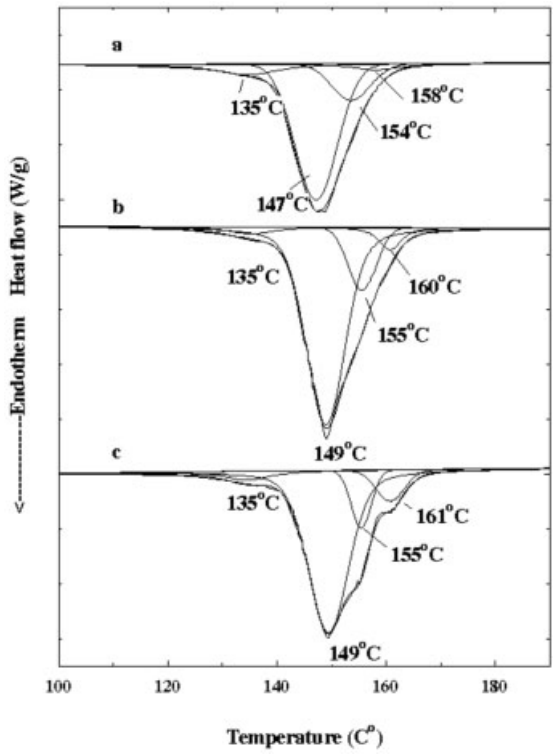

Figure 11 Resolved DSC thermograms of Dyneema® grade polyethylene fibers. (a) Dyneema® SK60; (b) Dyneema® SK65; (c) Dyneema® SK75. Peak positions are shown on the thermograms.

around 155–156°C, in the high temperature tail region. Using the two-phase modeling approach and using eq. (13), DSC fractional crystallinity values are evaluated and are listed in Table V. DSC fractional crystallinity values for the USA origin Spectra® grade PE fibers vary between 76 and 77% whereas Holland origin Dyneema® grade PE fibers show variation between 72 and 83%, respectively. As a result, the amorphous fraction varies between 17 and 28% for the USA and Holland origin PE fibers. Because of the limitations of the two-phase modeling approach where the third phase known as oriented noncrystalline structure is ignored altogether.

To overcome the limitations of the two-phase modeling approach, an alternative and independent approach is exercised. Assuming that the DSC thermograms contain no melting endotherms due to the amorphous phase and further assuming that the total melting enthalpy area in the 130–170°C region is due to the sum of the melting of folded lamellar crystals, polymorphic crystals containing orthorhombic and monoclinic phase and intermediate phase (i.e., oriented noncrystalline or pseudo hexagonal phase). We can further assume that the amorphous fractional component is the same as in the X-ray diffraction analysis.

Using the earlier mentioned assumptions, a well established curve fitting procedure[41] is employed to obtain fractional crystallinity values for each component. The fractional crystallinity known as peak area crystalinity is evaluated using eq. (14).

As shown in Figures 10 and 11, in all cases four endotherms, have been observed following the curve fitting procedure. The positions of the melting endotherms as determined from the peak resolution are presented in Table V. The melting peak positions are found to be in good agreement with those published previously.[10,18–20] Although not observed in the DSC thermograms of the present study shown in Figures 10 and 11, because of the temperature range covered being between 20 and 200°C, a glass transition temperature of 1.85°C was reported[20] for the USA origin Spectra® 900 and 2000 PE fibers. There is no doubt that similar transition temperature is likely to be expected for the Holland origin PE fibers. Furthermore, external restrains and annealing are reported to cause an increase in the melting temperature.[20]

According to the curve-fitting, the first and weak/broad endotherm is found to be located in the 135–136°C temperature range. This endotherm is assigned to the melting of the folded lamellar crystals.[10,18–20] The results from the curve fitting of the first melting endotherm suggest peak-widths ranging from 9 to 12°C for the USA and Holland origin PE fibers. The results also suggest a proportion of folded lamellar crystals between 3.4 and 11.8% for the USA origin and between 3.6 and 5.8% for the Holland origin PE fibers (see Table VI). It is suggested[15] that orthorhombic crystals possess two macro-conformations. The first

TABLE V
Thermal Analysis Results

Sample	T_{m1} (°C)	T_{m2} (°C)	T_{m3} (°C)	T_{m4} (°C)	ΔH (J/g)	χ_c (%) from DSC	χ_{am} (%) from DSC
SPECTRA® 900	135	146	153	159	222.2	76	24
SPECTRA® 1000	135	150	156	—	224.3	77	23
SPECTRA® 2000	136	150	157	—	225.9	77	23
DYNEEMA® SK60	135	147	152	164	211.1	72	28
DYNEEMA® SK65	135	149	155	160	243.4	83	17
DYNEEMA® SK75	135	149	155	161	242.0	83	17

TABLE VI
Fractional Components Obtained from Curve Fitting of DSC Traces

Sample	$\%\chi_1$ folded-chain lamellar crystals	$\%\chi_2$ orthorhombicphase	$\%\chi_3$ oriented intermediate (pseudo hexagonal phase)	$\%\chi_4$ monoclinic phase	DSC crystallinity $\Sigma\%\chi = \%\chi_1 + \%\chi_2 + \%\chi_4$	χ_{am} (%) amorphous phase-from X-ray analysis
SPECTRA® 900	11.8	42.2	32.0	11.0	65.0	3.0
SPECTRA® 1000	8.8	58.1	25.2	4.8	71.7	3.0
SPECTRA® 2000	3.4	73.2	19.0	2.3	78.9	2.0
DYNEEMA® SK60	5.8	66.7	16.2	4.3	76.8	7.0
DYNEEMA® SK65	4.0	71.8	14.5	5.7	82.1	4.0
DYNEEMA® SK75	3.6	75.0	11.4	9.6	88.2	5.0

macro-conformation is the lamellar crystals and the second macro-conformation is the extended-chain crystals. It is clear that high-modulus PE fibers appear to have relatively very low content of folded-chain crystals due to the unfolding processes taking place during the gel-spinning process.

The second and strong endotherm is found to be located in the 147—-149°C and 147–150°C temperature ranges for the Dyneema® and Spectra® grade PE samples, respectively. This endotherm is assigned to the melting of the commonly observed orthorhombic crystals.[10,18–20] Curve fitting results suggest orthorhombic peak-widths range from 8 to 10°C for the USA origin and 9 to 11°C for the Holland origin PE fibers. The results further suggest a proportion of orthorhombic crystals range from 42.2% to 73.2% for the USA origin and from 66.7 to 75% for the Holland origin PE fibers (Table VI).

Fu et al.,[15] using NMR analysis, evaluated orthorhombic crystallinity fractions of 73 and 64% for the research samples provided by Allied Signal Inc., with densities of 0.964 and 0.978 g/cm^3 and with Young's modulus of 179 and 59 GPa, respectively. Although their samples are not identical to the samples studied in the present investigation, still their results point to the right direction.

The shoulder shaped third endotherm is located in the 154–157°C temperature range and is assigned to the melting of oriented intermediate phase known as hexagonal mesophase[10,18–20] as a result of the transformation from the orthorhombic phase. Curve fitting results suggest hexagonal mesophase peak-widths showing variation between 11°C and 12°C for the USA and Holland origin PE fibers, respectively. The results suggest a proportion of hexagonal mesophase of 19–32% for the USA origin and 11.4–16.2% for the Holland origin PE fibers (Table VI). Hexagonal mesophase fractional values for the USA origin PE fibers are found to be in good agreement with the published results[18–20] where oriented hexagonal mesophase contents for the Spectra® 900 and 2000 grade PE fibers were found to be 30 and 33%, respectively.

The ratios of the melting enthalpy (or heat of fusion[18–20]) of hexagonal mesophase to the melting enthalpy of orthorhombic phase for the USA origin PE fibers are found to range from 25.9 to 75.8% and from 15.2 to 24% for the Holland origin PE fibers, respectively. Using thermal analysis, Kwon et al.[20] found the ratio of melting enthalpy of hexagonal phase to the melting enthalpy of orthorhombic phase to be 43% for the Spectra® 900 and 2000 fibers, respectively.

The fourth and weak endotherm is located in the 158–160°C temperature range and is commonly assigned to the melting of the monoclinic crystalline structure.[10,18–20] Curve fitting results for the monoclinic peak-widths showing variation between 11 and 13°C for the USA and Holland origin PE fibers. As shown in Table VI, monoclinic proportion varies between 2.3 and 11% for the USA origin and 4.3 and 9.6% for the Holland origin PE fibers, respectively.

Monoclinic fractional crystallinity values are in agreement with those published by Fu et al.[15] using NMR analysis, where they evaluated the monoclinic crystallinity fractions of 11 and 14%, respectively, for the research samples provided by Allied Signal Inc.

It seems that during the gel-spinning process, molecular chains are highly extended along the fiber axis direction whereby leaving only a small fraction of folded chain conformations forming folded lamellar crystallites. This process results in highly extended-chain conformations in the orthorhombic, monoclinic, and intermediate phases as a result of unfolding of lamellar crystallites and straightening of the amorphous chains taking place during the fiber production stages.

Analysis of Raman spectroscopy data

As mentioned before, the normalized peak area of crystalline band located at 1418 cm^{-1} has been used to determine the fractional Raman crystallinity of the polyethylene fibers under investigation. This peak is assigned[35] to the CH_2 bending mode due to the inter-

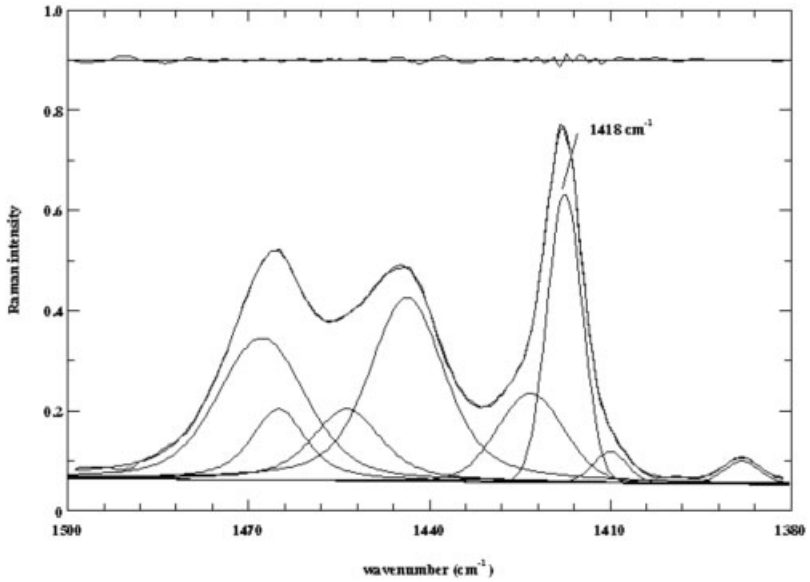

Figure 12 An example of the Raman spectrum peak resolution in the 1500–1380 cm^{-1} region. The lower curves are the fitted peaks, the middle curve is the observed spectrum, and the upper curve is the difference between the observed spectrum and the fitted spectrum on the same scale.

action between the two chains present in the orthorhombic unit cell.

As shown in Figure 12, the 1500–1380 cm^{-1} region has been fitted with eight peaks. Only the integrated intensity of the 1418 cm^{-1} peak has been used and the rest of the peaks are disregarded. Also, as shown in Figure 13, the 1350–1200 cm^{-1} region has been fitted with six peaks. In the calculations, the integrated intensities of 1312, 1296, and 1285 cm^{-1} have been added to give the normalization factor for the crystalline peak located at 1418 cm^{-1}. The results show that the bandwidth of crystalline band at 1418 cm^{-1} varies between 7.02 and 9.16 cm^{-1} whereas the bandwidth of the peak located at 1296 cm^{-1} varies between 6.7 and 7.15 cm^{-1}, respectively.

The Raman crystallinity values obtained from the Raman analysis for all the six samples are listed in Table VII and shown in Figure 14. The results show that the Raman crystallinity values vary between 66 and 79% for all the samples investigated. As a result, the amorphous fraction varies between 21 and 26% for the USA origin and 27 and 34% for the Holland origin PE fibers, respectively.

The crystallinity differences between the samples are relatively insignificant and all show relatively high values because of the high lateral chain packing attained during the fiber production stages. Raman crystallinity is also based on a two-phase modeling approach and assumes that the structure is composed of crystalline and amorphous phases thereby ignoring the presence of third phase known as intermediate or oriented noncrystalline phase.

Analysis of crystallinity values from density calculations

Using manufacturer's density values, i.e., 0.97 g/cm^3 for each sample, and using eq. (10) based on a two-phase modeling approach, the mass fractional crystallinity for each sample is identical and is equal to 78%. Therefore, the amorphous fraction is 22%. Another approach was to use the Lorentz densities, shown in Table I. As a result, the mass fractional crystallinity values, listed in Table VII, are found to vary between

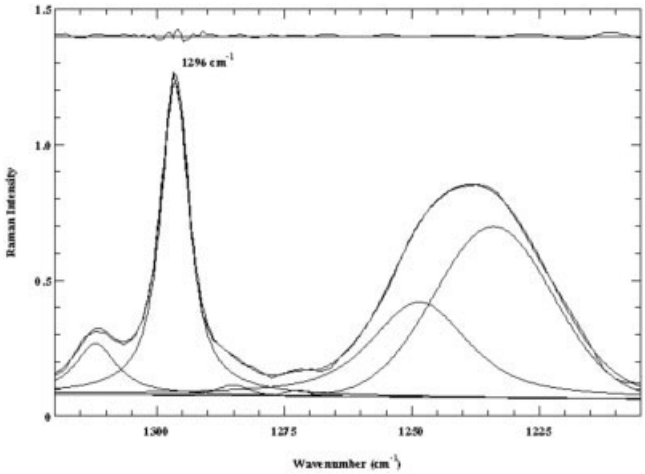

Figure 13 An example of the Raman spectrum peak resolution in the 1325–1205 cm^{-1} region. The lower curves are the fitted peaks, the middle curve is the observed spectrum, and the upper curve is the difference between the observed spectrum and the fitted spectrum on the same scale.

TABLE VII
Comparison of Crystallinity (χ_c) Measurements by Different Methods. χ_{am} Is the Amorphous Fraction

Sample	χ_c (%) from Lorenz density	χ_{am}(%)	χ_c (%) from curve fitting of DSC traces	χ_c(%) from Raman spectroscopy	χ_{am}(%)	χ_c (%) from IR spectroscopy	χ_c (%) from X-ray ortho+mono. See Table IV
SPECTRA[4]900	79.7 (78.0)[a]	20.3	65.0 (76)[b]	74	26	68	67
SPECTRA®1000	80.6 (78.0)[a]	19.4	71.7 (77)[b]	77	23	67	60
SPECTRA®2000	80.9 (78.0)[a]	19.1	78.9 (77)[b]	79	21	66	52
DYNEEMA® SK60	80.3 (78.0)[a]	19.7	76.8 (72)[b]	66	34	68	84
DYNEEMA® SK65	80.3 (78.0)[a]	19.7	71.0 (83)[b]	70	30	72	85
DYNEEMA® SK75	80.9 (78.0)[a]	19.1	88.2 (83)[b]	73	27	69	70

[a]The crystallinity values in brackets are evaluated using density values listed in Table I provided by the manufacturers.
[b]The crystallinity values in brackets are evaluated using two-phase model via eq. (13). See Tables V and VI for amorphous fractions.

79.7 and 80.9% for the USA based Spectra® grade PE fibers and between 80.3 and 80.9% for the Holland origin Dyneema® grade PE fibers. Amorphous fraction values obtained from Lorentz densities range between 19.1 and 20.3% for the USA and Holland origin PE fibers.

Fu et al.,[15] using a crystal density of 0.997 g/cm^3 and an amorphous density of 0.854 g/cm^3, arrived at the mass fractional crystallinities of 86 and 84% for the Spectra® 900 and 2000 grade PE fibers. Their high values appear to be the result of lower crystalline density and higher amorphous density than the values used in the present study.

The results also suggest that the mass fractional crystallinity values based on a two-phase modeling approach ignores the presence of oriented intermediate phase (i.e., oriented noncrystalline phase) and hence overestimates the true amorphous fraction. In the two-phase modeling approach, crystallinity values appear to include a smaller proportion of intermediate phase whereas the amorphous fraction appears to include larger fraction of intermediate phase. It is also true that the two-phase modeling also assumes constant amorphous density for the drawn samples where the amorphous density is expected to increase following the chain alignment.

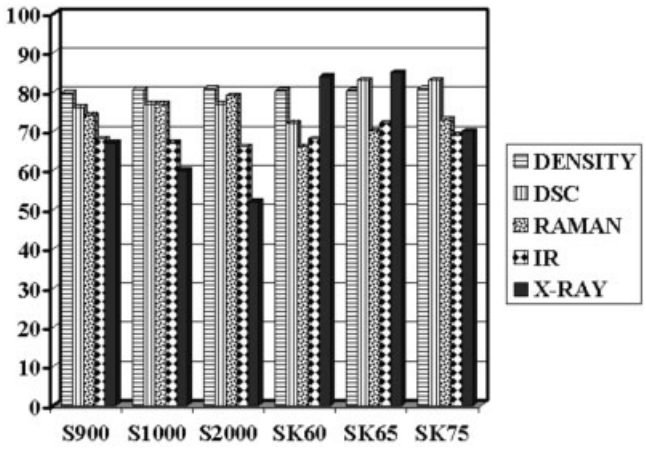

Figure 14 Comparison of crystallinity values obtained by various methods. S900, Spectra® 900; S1000, Spectra® 1000; S2000, Spectra® 2000; SK60, Dyneema® SK60; SK65, Dyneema® SK65; SK75, Dyneema® SK75.

Comparison of crystallinity values measured by different methods

In polymer and fiber science, the crystallinity is defined as the relative proportion of three-dimensionally organized structure and is most directly determined by X-ray diffraction analysis. The crystallinity values obtained from density, thermal, X-ray diffraction, infra-red, and Raman spectroscopy are listed in Table VII and compared in Figure 14. The results suggest that the crystallinity values determined from density and thermal analysis are generally close to each other for the Spectra® grade PE fibers but slightly different for Dyneema® grade PE fibers. On average, X-ray crystallinity values are slightly lower for the USA based PE fibers and higher for the Holland based PE fibers than the fractional crystallinity values obtained by other measurement methods.

X-ray diffraction method using data from equatorial region is often used to measure the lateral order parameter between a predefined angular region and is based on the separation of crystalline and noncrystalline scatter using curve fitting procedures. Although the X-ray procedure is more reliable than the other methods, it is still possible that the results may still

contain small amounts of oriented noncrystalline material, but this quantity is not expected to be very high.

In the case of vibrational spectroscopy including infra-red and Raman spectroscopy, the crystallinity values are based on the measurements of the content of the fully extended chain conformations. Normally, fully extended chain conformations contain trans conformers in the crystalline phase but it is also possible that trans conformers may also be present in the amorphous phase.

Normally, the density of the noncrystalline material increases with orientation. This means that the crysallinity measurements based on the use of constant noncrystalline density of amorphous material may contain high uncertainties when applied to the highly oriented samples. Normally, the samples with low crystallinites tend to have more reliable crystallinity values than the samples with high crystallinities because of the smaller changes in the amorphous density used in the calculations.

The thermal analysis data are most often complicated by the presence of crystallization exotherms taking place before the melting process in the samples with low crystallinity as well as the possible errors introduced during the formation of the baselines necessary for the calculation of areas. Since there is no crystallization exotherm seen in the DSC traces of the present highly oriented and crystalline PE fibers but the possibility of error still remains in the positioning of the baselines for area calculation. Despite this possibility, this uncertainty is expected to be small.

In all cases, if we assume that the most accurate evaluation of amorphous fraction is obtainable from X-ray diffraction analysis, the amorphous fraction obtained from density, thermal analysis, and Raman spectroscopy methods based on a two-phase modeling approach appears to be overestimated and appears to include larger proportion of intermediate phase whereas the crystallinity measurements from the same methods appear to include smaller proportion of intermediate phase.

CONCLUSIONS

Molecular structure and orientation of commercially available polyethylene fibers have been investigated utilizing optical microscopy, X-ray diffraction, thermal analysis, infra-red, and Raman spectroscopy techniques, with the aim of carrying out detailed structural characterization. The results obtained from six fiber samples of different origin are compared and discussed in terms of molecular orientation, structure, and the degree of order. Owing to the unavailability of the processing conditions because of commercial reasons, unfortunately, no definite processing-structure-property relationships can be established at present.

The results from the birefringence measurements show that the gel-spun polyethylene fibers consist of highly aligned chains along the fiber axis direction. Thermal analysis and wide-angle X-ray diffraction analysis involving the equatorial scatter show that the polyethylene fibers contain polymorphic crystallites arising from regular packing of orthorhombic and monoclinic structures. The chains emerging from the polymorphic crystalline phase form highly aligned pseudohexagonal structure with larger chain separation distances and chain cross-sectional areas than the orthorhombic and monoclinic crystallites.

Measurements carried out at room temperature suggest the presence of a three-phase structure consisting of polymorphic crystallites (orthorhombic and monoclinic phases), oriented noncrystalline, and unoriented noncrystalline (amorphous) phases. The results obtained from density, thermal analysis, and Raman spectroscopy based on a two-phase modeling approach suggests an overestimated amorphous fraction while ignoring the presence of a third phase known as intermediate phase. It appears that the amorphous fraction from two-phase modeling approach includes larger proportion of intermediate phase whereas the crystallinity measurements from the same techniques appear to include smaller proportion of intermediate phase.

Detailed investigation of crystallite size measurements involving the highly diffracting,(110),(200), and (020) reflections suggest that the USA based polyethylene fibers contain an average of 1360 laterally packed polymer chains whereas the Holland based polyethylene fibers contain an average of 725 laterally packed polymer chains due to the smaller sized crystallites. This means that the USA based PE fibers contain more laterally ordered chains than the Holland based PE fibers. Enhanced lateral chain packing is expected to lead to improved mechanical properties in terms of enhanced tensile strength and modulus.

The use of polarized IR spectroscopy has been very useful in establishing the orientation parameters of crystalline and oriented noncrystalline phases. The IR peak at 730 cm^{-1} has yielded the crystalline orientation parameter of the orthorhombic phase whereas the splitting of the 718 cm^{-1} IR peak yielded the orientation parameters of the monoclinic phase and oriented pseudohexagonal noncrystalline phase, respectively. Although, smaller in quantity, the monoclinic crystallites are found to be more oriented than the dominant orthorhombic crystallites. The results show that the orthorhombic and monoclinic phases are more highly oriented than the oriented pseudohexagonally packed noncrystalline chains.

Because of the ability of the X-ray diffraction method, it has been possible to differentiate between the polymorphic crystalline and noncrystalline structures. With this technique, it has been possible to

determine the crystallinity of the orthorhombic and monoclinic phases, respectively. The results from the curve-fitting analysis of the equatorial scatter show that the unoriented noncrystalline structure, because of the high molecular orientation and well-formed lateral packing, is very small in quantity and varies between 2 and 3% for the USA based PE fibers and between 4 and 7% for the Holland based PE fibers. Further analysis of the results point to the fact that the USA based polyethylene fibers appear to have more oriented hexagonal mesophase content of 30–46% than the Holland based polyethylene fibers (with variation between 9 and 25%). The differences between the content of the oriented hexagonal mesophase is attributed to the possibility of different processing conditions employed during the manufacturing stages.

The author thanks DSM of Holland and Allied Signal Inc (now part of Honeywell International Inc.) for the supply of the samples investigated in the present study. Thanks also go to Volkan Unsal for the assistance with the data collection. Special thanks go to an anonymous reviewer for making useful comments.

References

1. Keller, A. Rep Prog Phys 1968, 31, 623.
2. Capaccio, G.; Ward, I. M. Polymer 1974, 15, 233.
3. Capaccio, G.; Ward, I. M. Polymer 1975, 16, 239.
4. Anonim. High Performance Textiles 1985, 6, Number 1, July.
5. http://www.spectrafiber.com.
6. http:// www.dsm.com.
7. Smith, P.; Lemstra, P. J. J Mat Sci 1980, 15, 505.
8. Lemstra, P. J.; Kirschbaum, R. Polymer 1985, 26, 1372.
9. Stein, R. S.; Norris, F. H. J Poly Sci 1956, 21, 381.
10. Hsieh, Y.-L.; Hu, X.-P. J poly Sci: Part B: Poly Phys 1997, 35, 623.
11. Mahendrasingam, A.; Blundell, D. J.; Wright, A. K.; Urban, V.; Naarayanan, T.; Fuller, W. Polymer 2004, 45, 5641.
12. Walter, E. R.; Reading, F. P. J Polym Sci 1956, 21, 561.
13. Bunn, C. W. Trans Faraday Soc 1939, 35, 42.
14. Swan, P. R. J Polym Sci 1962, 56, 403.
15. Fu, Y.; Chen, W.; Pyda, M.; Londono, D.; Annis, B.; Habenschuss, A.; Cheng, J.; Wunderlich, B. J Macromol Sci Phys 1996, 35, 37.
16. de Vries, H. Colloid & Polym Sci 1979, 257, 226.
17. Hamza, A. A.; Sokkar, T. Z. N.; Mabrouk, M. A.; El-Morsy, M. A. J Appl Poly Sci 2000, 77, 3099.
18. Hu, W.; Buzin, A.; J-S Lin; Wunderlich, B. J Poly Sci Part B: Poly Phys 2003, 41, 403.
19. Pak, J.; Wunderlich, B. Thermochimica Acta 2004, 421, 203.
20. Kwon, Y. K.; Boller, A.; Pyda, M.; Wunderlich, B. Polymer 2000, 41, 6237.
21. Wunderlich, B. Macromolecular Physics 1980, 3, 69.
22. Cheng, J.; Fone, M.; Fu, Y.; Chen, W. J Therm Anal 1996, 47, 673.
23. Smith, J. B.; Manuel, A. J.; Ward, I. M. Polymer 1975, 16, 57.
24. Chen, W.; Fu, Y.; Wunderlich, B.; Cheng, J. J Polym Sci Polym Phys 1994, 32, 2661.
25. Krimm, S. Fortschr Hochpolym–Forsch 1960, 2, 51.
26. Read, B. E.; Stein, R. S. Macromolecules 1968, 1, 116.
27. Kaito, A.; Nakayama, K.; Kanetsuna, H. J Macromol Sci 1987, B26, 281.
28. Krishnaswamy, R. K. J Polym Sci, Part B: Polym Phys 2000, 38, 182.
29. Snyder, R. G. J Chem Phys 1979, 71, 3229.
30. Snyder, R. G.; Maroncelli, M.; Strauss, H. L.; Hallmark, V. M. J Chem Phys 1986, 90, 5623.
31. Furuheim, K. M.; Axelson, D. E.; Antonsen, H. W.; Helle, T. J Appl Poly Sci 2004, 91, 218.
32. Kang, N.; Xu, Y.-Z.; Cai, Y.-L.; Li, W.-H.; Weng, S.-F.; Feng, W.; He, L.-T.; Xu, D.-F.; Wu, J- G.; Xu, G.-X. J Mol Struc 2001, 562, 19.
33. Lu, S.; Russell, A. E.; Hendra, P. J. J MatSci 1998, 33, 4721.
34. Paradkar, R. P.; Sakhalkar, S. S.; He, X.; Ellison, M. S. J Appl Poly Sci 2003, 88, 545.
35. Lagaron, J. M. J Mat Sci 2002, 37, 4101.
36. Ohta, Y.; Kaji, A.; Sugiyama, H.; Yasuda, H. J Appl Poly Sci 2001, 81, 312.
37. Green, D.; Bower, D. I. Spectrochemica Acta 1993, 49A, 1191.
38. Karacan, I.; Taraiya, A; Bower, D. I.; Ward, I. M. Polymer 1993, 34, 2691.
39. Karacan, I.; Bower, D. I.; Ward, I. M. Polymer 1994, 35, 3411.
40. Bozdogan, F.; Karacan, I.; Kitagawa, T. J Mat Sci Tech 2000, 8, 119.
41. Hindeleh, A. M.; Johnson, D. J; Montague, P. E. In Fiber Diffraction Methods; French, A. D., Gardner, K. H. Eds.; ACS Symposium Number 141; American Chem Society: Washington, DC, 1983; p 149.
42. Stokes, A. R. Proc Phys Soc 1948, A166, 283.
43. Jarvis, D. A.; Hutchinson, I. J.; Bower, D. I.; Ward, I. M. Polymer 1980, 21, 41.
44. Hindeleh, A. M.; Johnson, D. J. Polymer 1978, 19, 27.
45. Zhang, H.; Shi, M.; Zhang, J.; Wang, S. J Appl Poly Sci 2003, 89, 2757.